ratur von 56 °C das Wasser von der höheren zur tieferen Temperatur wandert. Dieses Resultat ist nicht unvernünftig, weil alle Messungen des Thermodiffusionsfaktors α_T bei hochmolekularen Lösungen zeigen, daß mit zunehmender Konzentration des Hochpolymeren die (positive) Größe α_T rapide abnimmt und im hochviskosen Bereich (in dem Messungen der Thermodiffusion unmöglich sind) wahrscheinlich negativ wird. Allerdings liegt bei gequollener Cellulose keine normale hochmolekulare Lösung, sondern ein binäres gummielastisches System mit vernetztem Hochpolymeren vor.

Nach den Daten in Tab. 2 gilt nun: $\varrho_M/\varrho \approx 1{,}7$. Demnach ist die Grundvoraussetzung (16) für unser System nicht erfüllt. Auch die Annahme einer reinen Löslichkeitsmembran ist also nicht berechtigt.

Schlußbetrachtungen

Cellophanfolien in Wasser sind offensichtlich weder Poren- noch Löslichkeitsmembranen, sondern wahrscheinlich eine Kombination dieser beiden Grenztypen. Unter diesen Umständen ist eine quantitative Deutung der gemessenen Transportgrößen A und B (und Q^*) äußerst schwierig.

Wir werden – nach Vollendung der im Gang befindlichen Untersuchungen am System Cellophan + Methanol – Messungen an der Permeation und Thermoosmose von reinen Flüssigkeiten durch Niederschlagsmembranen (Cellophanfolien mit Kupferferrocyanid) durchführen. Hier dürfte mit einem Überwiegen des Mechanismus der Löslichkeitsmembran zu rechnen sein, so daß die Beziehungen (17) und (18) von Nutzen sein könnten.

Experimental Evidence of Clusters in Molten Alloys of the Eutectic Aluminum-Tin System by Means of a X-Ray-high Temperature-small Angle Scattering Apparatus

R. Hezel and S. Steeb

Max-Planck-Institute for Metal Research, Institute for Refractory Metals, Stuttgart, Germany

(Z. Naturforsch. **25 a**, 1085—1091 [1970]; received 26 February 1970)

An apparatus for measuring X-Ray small- and wide angle scattering of solid materials and especially of molten metals with temperatures up to 1100 °C is described. Alloys of the eutectic system Al—Sn with tin-contents up to 30 At.-% are investigated. The influence of surface oxide layers on the scattered intensity is discussed. Correlation functions as well as the Guinier approximation yielded inhomogeneities with mean diameters up to 10 Å in the investigated melts. Therefore the dimensions of these so-called short range segregation zones correspond to those of the first coordination sphere.

§ 1. Introduction

To investigate the structure of molten metals and alloys until now scattering of X-Rays, electrons and neutrons was studied in the wide angle region exclusively. The result of nearly oll of these experiments was the evaluation of the atomic distribution from measured scattering curves. In this way a decision could be obtained whether short range order, short range segregation or statistical distribution of the atoms exists. In many papers dealing with these structural data and other physical properties of melts (e. g. viscosity, electrical resistivity, and thermodynamical measurements) it was concluded in an indirect way, that in certain molten alloys agglomerates of atoms exist, which in their structure are similar to the atomic arrangements in the corresponding solid state. In the present paper a direct evidence of inhomogeneities is given. For the first time the method of X-Ray small angle scattering was applied to metallic melts for this purpose. By such experiments it is possible to obtain quantitative information on size and shape of particles with diameters of about five to some thousand Å-units. To get small angle scattering at all, a difference in electron density between the particles and their surroundings must exist. To obtain sufficient intensity, the system aluminum-tin was chosen. In the solid state, this system shows only small mutual solubility of the two components. Furthermore there is a relatively high difference in electron density between the two components.

Since the performance of X-Ray small angle scattering experiments with molten metals by the aid of commercially available equipments is impossible, a special apparatus had to be designed. Additio-

Sonderdruckanforderungen an Priv.-Doz. Dr. S. Steeb, Max-Planck-Institut für Metallforschung, *D-7000 Stuttgart-1*, Seestr. 92.

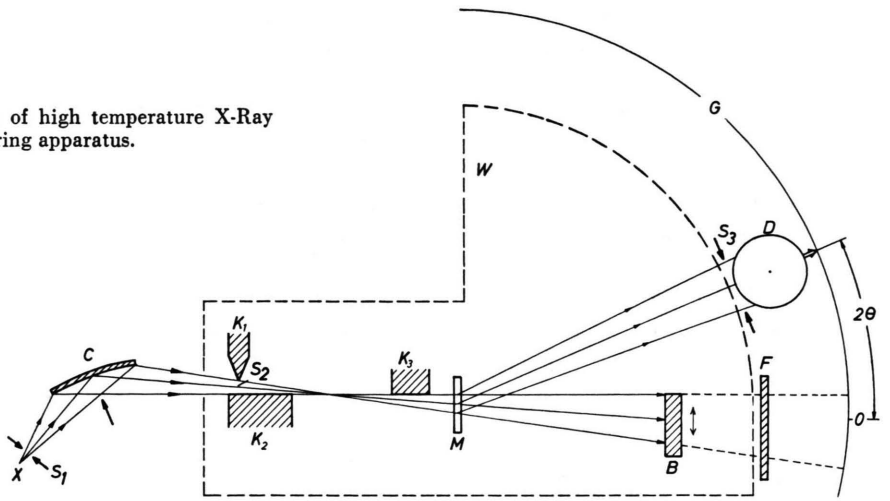

Fig. 1. Schematic representation of high temperature X-Ray small angle scattering apparatus.

nally, with this apparatus to be described in the next chapter, it is possible to investigate simultaneously the wide angle region.

§ 2. Experimental Details

Fig. 1 shows the schematic arrangement of the apparatus. The X-Rays emerging from the focus X of the X-Ray tube pass through the slit S_1 and are made monochromatic by reflection at a crystal C (Johann-type, quartz). Then they pass through an entrance window (mylar foil) into the recipient whose walls are watercooled. The so called Kratky camera (K_1, K_2, and K_3) defines the beam in such a way that the region behind K_3 remains free of parasitic scattering, especially in the field above the plain given by K_2 and K_3. The camera was made of one block of stainless steel and can be adjusted during the experiment from outside the recipient by two micrometer screws (translation and rotation). Furthermore the camera temperature is kept constant by water cooling. This is necessary, because immediately behind K_3 a furnace with the melt M under investigation follows. This furnace was built of nickel and is heated by molybdenum wire. The temperatures attainable amount up to 1100 °C. The melt under investigation is contained in a cuvette of mica or beryllium foils. It is of importance, that the cuvette can be withdrawn from the beam by a manipulator from outside during the experiment, i. e. under vacuum or protecting gas atmosphere. Herewith it is possible to measure the intensity of the primary beam. To avoid corrosion at higher temperatures, the choice of the cuvette material has to be done according to the special alloy under investigation. The X-Rays, scattered at an angle of 2Θ versus the primary beam are recorded by the proportional counter D followed by a pulse height discriminator. The counter moves on the goniometer circle G. As origin 0 of angle scale the position of maximum intensity of the primary beam was chosen. Angles 2Θ from 10′ to 70° can be detected by this experimental arrangement. It should be mentioned, that the resolution of the apparatus described is still higher, if strong scatterers are used. With a polyethylene sample for example, 2Θ-values down to 4′ can be obtained.

The beam stop B made of molybdenum foil protects the counter from the direct beam without causing any additional scattering and without producing any shadow in the small angle region itself. To avoid air scattering, the beam stop must be located inside the chamber. Exact adjustment of the beam stop can be done during the experiment from outside the apparatus by a micrometer screw.

The measurements were done under Helium-atmosphere for reduction of background scattering. The absorption foil F is used for the measurement of the primary beam intensity. This measurement is necessary to determine the absorption and thickness of the melt, respectively. By repeated measuring of the primary beam intensity, weakened by the specimen, it is also possible to pursue geometrical changes of the melt during the experiment. Of course it is also possible to observe changes in primary intensity itself by removing the specimen with the manipulator described above. This equipment also allows the determination of the so called "absolute" scattered intensity, i. e., the ratio of intensity scattered by the specimen and the primary intensity having passed the specimen. The use of calibrated absorption foils for these purposes is justified because of the strictly monochromatic primary beam.

§ 3. Evaluation of Small Angle Scattering Diagrams

Fig. 2 shows the continuous change from wide angle- (W) to small angle (S)-scattering: The part marked with W shows the usual shape of an intensity curve for amorphous solids and for liquids. It is caused by the mutual arrangement of the atoms. If the specimen is homogeneous, i. e. if there are

no agglomerates of atoms (clusters), then for the small angle region the dash-dotted line would result. If, however, clusters exist in the specimen,

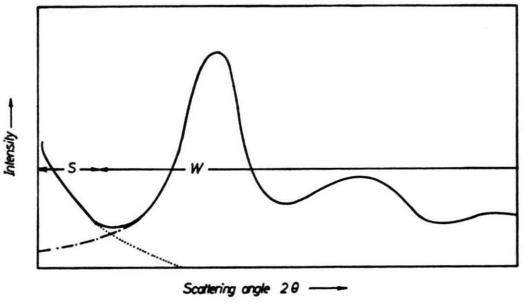

Fig. 2. Schematic representation of small- and wide-angle scattered intensity of molten alloys.

whose electron density is different from that of the surroundings, then small angle scattering S occurs, which ends at the smallest detectable angle $2\,\Theta_{\min}$ near the primary beam.

The theoretical treatment of small angle scattering (GUINIER and FOURNET [1], GEROLD [2, 3]) will only be considered so far as it is necessary for the evaluation of the experiments. We start from an equation given by GUINIER [1], according to which for diluted systems the angular dependence of small angle scattering can be described approximately by a Gaussian distribution curve:

$$I(s) = I(0) \cdot \exp\left(-\frac{R_s^2 \cdot s^2}{3}\right) \qquad (1)$$

with

$I(s)$ = small angle scattering intensity,
$I(0)$ = small angle scattering intensity extrapolated to $2\,\Theta = 0$,
R_s = radius of gyration $= \frac{1}{v}\int r^2\,\mathrm{d}v$,
v = volume of a particle,
r = distance of volume element $\mathrm{d}v$ from the center of gravity of electron mass.

The radius of gyration can be calculated for different shapes of particles. For spherical particles with radius R the following stands:

$$R_s = \sqrt{3/5}\,R\,.$$

From Eq. (1) follows:

$$\log I = -0.14\,R_s^2\,s^2 + \text{const}\,. \qquad (2)$$

Eq. (2) is the fundamental expression of the so called Guinier-method:

Plotting $\log I$ versus s^2 yields a straight line, the slope of which gives the radius of gyration R_s.

Another way for the determination of the approximate size of particles is represented by the function $\gamma_0(r)$, called correlation function by DEBYE and BUECHE [4] and characteristic function of a particle by POROD [5]. This function γ_0 follows from the angle dependent part $I(s)$ of the scattering intensity by Eq. (3):

$$\gamma_0(r) = \frac{K}{r}\int_0^\infty s \cdot I(s) \cdot \sin s\,r \cdot \mathrm{d}s\,. \qquad (3)$$

$\gamma_0(r)$ represents the probability that a point at a distance r in an arbitrary direction from a given point in the particle will itself also be in the same particle. At $r = 0$ $\gamma_0(r)$ has the value unity, which is achieved by the normalisation constant K in Eq. (3). γ_0 decreases with increasing r and becomes zero beyond the value $r = 2\,R$, which corresponds to the longest line through the particle. So the function γ_0 represents a possibility to determine the dimensions of a particle at least in a qualitative way.

§ 4. Experiments and Results *

1. Small angle scattering intensity curves from molten Al – Sn alloys

With the apparatus described in § 2 some molten alloys of the simple eutectic system Al – Sn (HANSEN and ANDERKO [6]) up to a tin content of 30 At.-% were investigated in the small angle region using Mo-Kα-radiation. The resulting intensity curves are shown in Fig. 3. The intensity is expressed in electron units, which is achieved by matching the measured curves to the mean atomic scattering factor in the wide angle region at the largest values of the abscissa $s = 4\pi(\sin\Theta/\lambda)$, with λ = wavelength of radiation used. The temperatures for the alloys with 3, 6, 10, 15, 30 At.-% Sn, respectively, amounted to

[1] A. GUINIER and G. FOURNET, Small Angle Scattering of X-Rays, J. Wiley & Sons, Inc., London 1955, Chapman & Hall, Ltd.
[2] V. GEROLD, Z. Elektro-Chemie **60**, 405 [1956].
[3] V. GEROLD, Z. Angew. Physik **9**, 45 [1957].
[4] P. DEBYE and A. M. BUECHE, J. Appl. Phys. **20**, 518 [1949].
[5] G. POROD, Kolloid-Z. **124**, 83 [1951].

* R. HEZEL, Kombinierte Untersuchungen der Kleinwinkel- und Weitwinkelstreuung von Röntgen-Strahlen an Aluminium und Aluminium-Zinn-Legierungen im schmelzflüssigen Zustand, Dissertation, Universität Stuttgart 1968.
[6] M. HANSEN and K. ANDERKO, Constitution of Binary Alloys, McGraw-Hill, New York 1958, p. 135.

658°(20°), 652°(25°), 650°(30°), 640°(20°), and 640°(50°) C. (The numbers in brackets always denote the temperature difference between the temperature of measurement and liquidus temperature.) From Fig. 3 it can be seen that the investigated al-

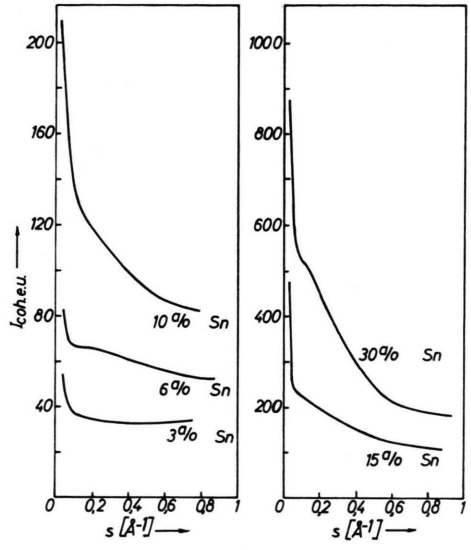

Fig. 3. Small angle scattering intensity in electron units of five molten alloys in the system Al—Sn.

loys show small angle scattering, which starting from pure aluminum increases with increasing tin content. Similar curves, extending over such a relatively large angle range up to now only were observed in the course of X-Ray investigations of the so called critical opalescence of Argon (THOMAS and SCHMIDT [7], EISENSTEIN and GINGRICH [8]), of Nitrogen (WILD [9]), of Helium I and II (TWEET [10]), and finally of Neon (STIRPE and TOMPSON [11]).

The small angle scattering curves continuously change over into the wide angle curves without becoming zero before ascending to the first maximum of the wide angle region. Because of this fact the separation of the two parts of the scattering curve is very difficult.

For experimental reasons it is impossible to measure the intensity curve over the whole angle range by one run. Therefore Fig. 4 shows the scattered intensity curve composed of three overlapping regions I, II, and III for a melt containing 15 At.-% tin.

The wide angle region (I) extends from $2\Theta = 1°$ to 65°, the region II from 20′ to 6° and the region III finally from 10′ to 1°. The width of entrance- and counter slits was reduced by passing from region I to region III. Count preset was used, the number of counts being 10 000 for each data point. The time for the performance of one experiment must be as short as possible for the following reasons: evaporation of specimen, reaction of the melt with the cuvette, and deformation of cuvette caused by the high temperatures necessary for the investigation of molten metals.

2. *Influence of the scattering of surface layers*

In Fig. 4 a pronounced increase of scattered intensity at small angle occurs. The investigations described below showed, that this effect is caused by

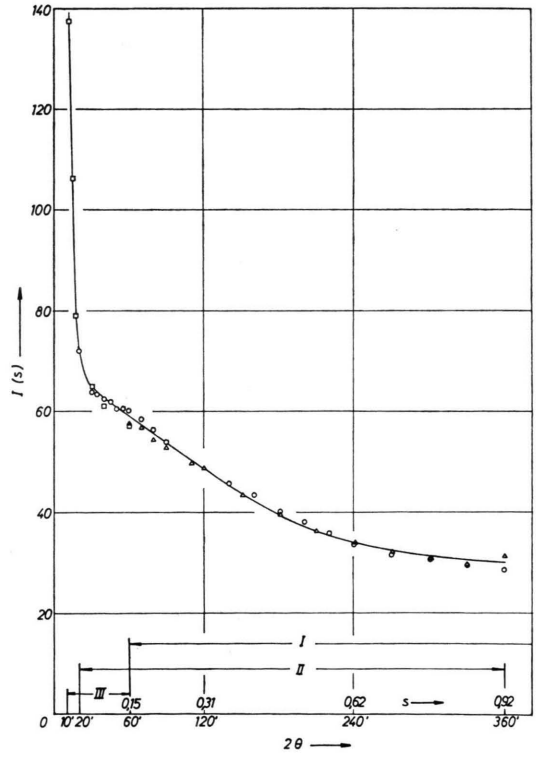

Fig. 4. Small angle scattering intensity of a molten alloy of Al with 15 At.-% Sn. △ = region I; ○ = region II; □ = region III.

[7] I. E. THOMAS and P. W. SCHMIDT, J. Chem. Phys. **39**, 2506 [1963].
[8] A. EISENSTEIN and N. S. GINGRICH, Phys. Rev. **62**, 261 [1942].
[9] R. L. WILD, J. Chem. Phys. **18**, 1627 [1950].
[10] A. G. TWEET, Phys. Rev. **91**, 488 [1953].
[11] D. STIRPE and C. W. TOMPSON, J. Chem. Phys. **36**, 392 [1963].

oxide layers always present on the surface of aluminum and its alloys.

By the following method it could be deciced, whether scattering arises from the volume or from the surface of the specimen. If the beam is scattered by the volume of the sample, then for the so called volume scattering I_v the relation stands:

$$I_v \approx d \cdot e^{-\mu d} \tag{4}$$

with d = thickness of the specimen, μ = absorption coefficient.

If however the scattering arises from the surface of the specimen, there is no linear dependence of scattered intensity from specimen thickness:

$$I_s \approx e^{-\mu d} \tag{5}$$

with I_s = intensity scattered from the surface of the specimen.

Measuring of the scattered intensities I_1 and I_2 of two specimens with thickness d_1 and d_2 yields under the same experimental conditions at a certain angle in the case of volume scattering

$$I_1/I_2 = (d_1/d_2)\ e^{-\mu(d_1-d_2)} \tag{6}$$

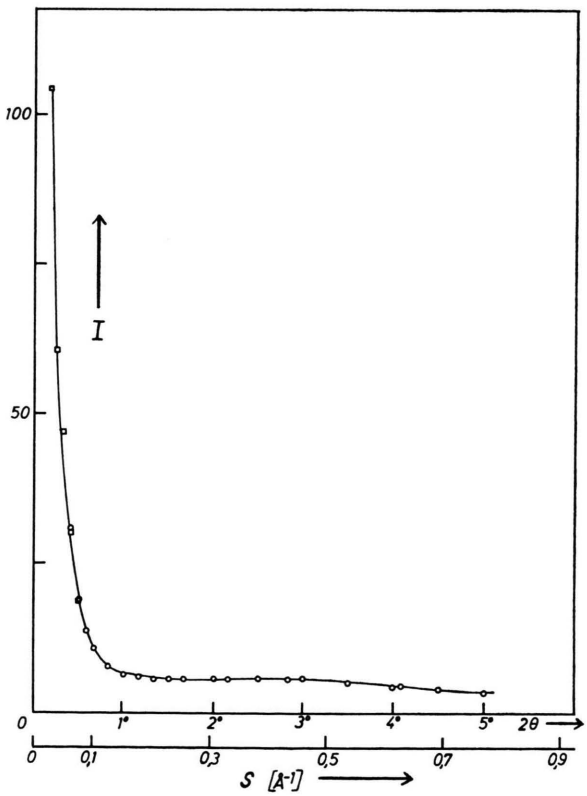

Fig. 5. Small angle scattering intensity of the surface layer of the molten alloy Al with 30 At.-% Sn.

and in the case of surface scattering

$$I_1/I_2 = e^{-\mu(d_1-d_2)}\ . \tag{7}$$

For the investigated alloys the validity of Eq. (7) could be confirmed, i. e., the strong scattering at very small angles is caused by surface layers.

Furthermore the scattering of surface layers was measured: The solid specimen of the corresponding alloy was fixed in an iron frame with an open end at the bottom and then heated up in the apparatus under the same conditions as applied in an actual experiment. After melting the liquid metal dropped down out of the X-Ray beam, the two oxide surface layers remained alone and their scattering could easily be investigated. For an alloy containing Al and 30 At.-% Sn the result is shown in Fig. 5. It can be recognized at once, that the pronounced increase of scattered intensity at small angles is similar to that shown in Fig. 4. Also at larger angles the surface layers contribute to the scattered intensity.

3. Determination of correlation function

Without assuming special assumptions about the structure of the system, i. e. independent whether a dilute or dense packed system is under investigation, or whether the shape of particles is spherical, elliptical or more complicated, with the characteristic function introduced in § 3 general conclusions can be deduced about the size of the present inhomogeneities. Calculating this function according to Eq. (3) it must be taken into consideration, that the upper limit of the integral is "infinite" and therefore a run of the curve of scattered small angle intensity as shown in Fig. 2 by the dotted line has to be assumed.

The shape of this part of the scattering curve only can be given arbitrarily at the moment. Since this part of the curve becomes more important than the part at small angles by multiplication with s in Eq. (3), the function $\gamma_0(r)$ can only be of qualitative significance.

In Fig. 6 is shown the function $\gamma_0(r)$ normalized to the value 1 at $r = 0$ for the alloy containing Al with 25 At.-% Sn. As mentioned in § 3, that value of abscissa, for which γ_0 becomes zero or very small, gives the approximate size of particles. All melts investigated show values $2R$ from 6 to 9 Å. By this figures the order of magnitude of the size of the particles is roughly given.

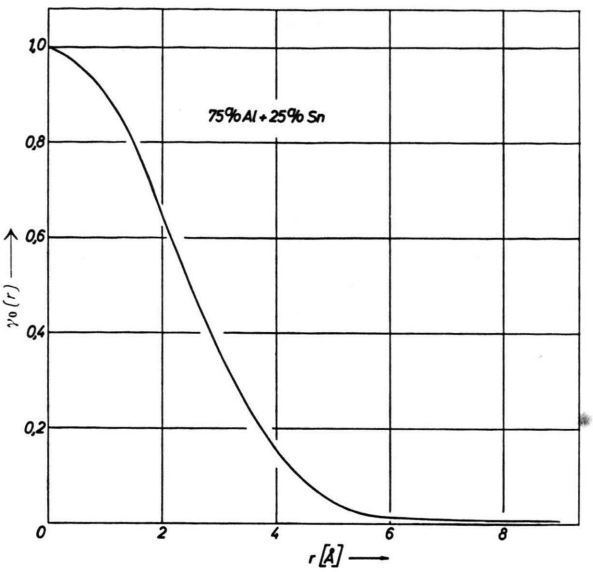

Fig. 6. Correlation function $\gamma_0(r)$ of the molten alloy Al with 25 At.-% Sn.

A more exact method for the determination of the size of particles is given by the Guinier approximation treated in the following chapter.

4. Guinier's Approximation

The Guinier approximation described in § 3 is valid for dilute systems only, i. e. for systems whose particles are arranged so far from each other, that no interparticular interference occurs, which possibly might disturb the particle scattering at small angles. That part of the scattering curve at very small angles, necessary for the application of Guinier's approximation, is influenced by the surface layer scattering mentioned in § 4.2 to such a degree that it cannot be used for evaluation at all. Since the large angle part of the small angle region is disturbed by the atomic scattering, in the present case Guinier's approximation only can be applied in the range $1° < 2\Theta < 2° 30'$.

Fig. 7 shows the Guinier plots of the molten Al-alloys containing 10 and 25 At.-% Sn, respectively and the straight lines touching these curves in the range mentioned above. For each of the investigated alloys the radius of gyration was determined from the slope of the tangents according to Eq. (2). This value was used to calculate the radii of particles, whose shape was assumed to be spherical. The resulting sphere diameters are plotted in Fig. 8 versus the tin-concentration. The limits of error marked at each point by a vertical line are determined by inaccuracies as neglecting of slit correction, influence of surface layer- and atomic-scattering and errors in matching the tangent to the Guinier plot (see Fig. 7).

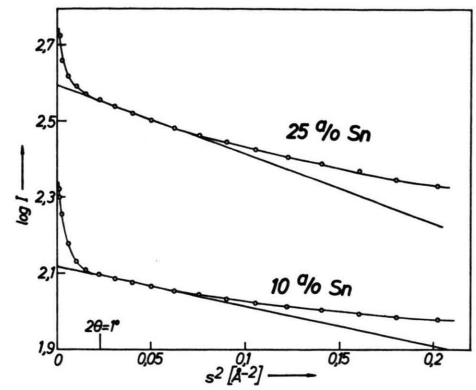

Fig. 7. Guinier plot of the scattering curves of two molten Al—Sn alloys.

It can be assumed with high probability, that the diameters of the particles existing in the molten Al—Sn alloys lie between the two dashed lines in Fig. 8.

§ 5. Discussion

In Fig. 8 the different values of particle diameters versus concentration show, starting from pure aluminum up to 20 At.-% Sn an increase in diameter

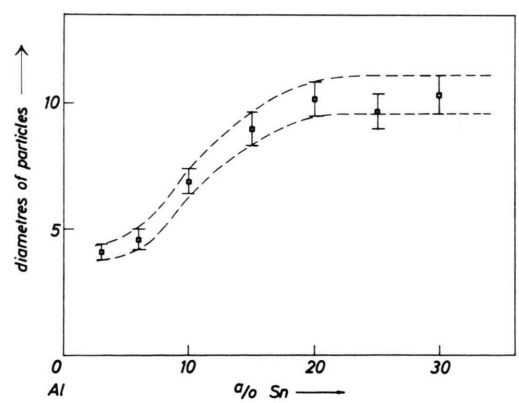

Fig. 8. Diameters of the inhomogeneities of Al—Sn melts.

up to 9 to 10 Å, which remains constant up to 30 At.-% Sn. These facts for example could be explained in the following way: By adding tin to an aluminum melt, a certain amount of tin atoms will be distributed statistically, according to the solubility in the liquid state, which probably exceeds that of

the solid state given by ELLIOTT [12]. With increasing tin content the first coordination spheres of the tin atoms are continuously filled up by tin atoms. At a tin concentration of about 15 to 20 At.-% coordination spheres are formed which mainly consist of tin atoms and are of spherical shape with a diameter of approximately three atomic diameters (9 – 10 Å). The small angle scattering caused by these particles does not change within the measuring time of two hours. From these considerations it can be concluded that the particles, whose existence was proved by the present work for the first time, form the so called short range segregation regions which extend upon one coordination sphere in the melt.

The constitution diagram of the simple eutectic system Al – Sn (HANSEN and ANDERKO [6]) doesn't show any immiscibility gap in the liquid region, so that the two kinds of atoms ought to be miscible at each concentration. Therefore the melts in the region above the liquidus until now were regarded to be homogeneous. From § 4.4, however, results that the alloys investigated show a "microheterogeneous" structure at least up to 100 °C above the liquidus. This experimental fact is confirmed by the extremely flat run of the liquidus with its pronounced point of inflection. Furthermore this tendency is expressed in the positive values of the heat of mixing with a maximum of $\Delta H = 970$ cal/g·atom (WITTIG and KEIL [13]). Also the isotherms of thermodynamic activity of aluminum and tin in molten Al – Sn alloys at 727 °C show a positive deviation from Raoult's law (OELSEN et al. [14]). This fact also shows the strong segregation tendency in Al – Sn melts.

Finally, the paper of BUBLIK and BUNTAR [15] should be mentioned, which indirectly derived from electron diffraction experiments a tendency for segregation into regions enriched with the atoms of one component in Al – Sn melts.

[12] R. P. ELLIOTT, Constitution of Binary Alloys, First Supplement, McGraw-Hill, New York 1965.
[13] F. E. WITTIG and G. KEIL, Z. Metallkde. **54**, 576 [1964].
[14] W. OELSEN, P. ZÜHLKE, and O. OELSEN, Arch. Eisenhüttenwesen **29**, 799 [1958].
[15] A. J. BUBLIK and A. G. BUNTAR, Fiz. Met. i Metalloved. **6**, 692 [1958].

Intramolekulare Excimere: Die Kinetik ihrer Bildung und Desaktivierung

WALTER KLÖPFFER und WOLFGANG LIPTAY

Battelle-Institut e. V., Frankfurt (Main) und Institut für Physikalische Chemie der Universität Mainz

(Z. Naturforsch. **25 a**, 1091—1096 [1970]; eingegangen am 6. Mai 1970)

A set of kinetic equations has been developed which allows to calculate the rate parameters of intramolecular excimer formation, dissociation and of radiative and non-radiative desactivation processes. Experimental data necessary for evaluating the equations are monomer lifetime and relative fluorescence intensities of monomer and excimer fluorescence in solution with and without added quenching substance.

Spectroscopical data of biscarbazolyl propane, diphenyl propane and derivatives are used in order to calculate the rate constants. It is shown that the stronger excimer fluorescence of diphenyl propane, as compared with biscarbazolyl propane, is due to the high rate constant of excimer formation in the former substance.

1. Einleitung

Intramolekulare Excimerfluoreszenz wurde erstmals von HIRAYAMA [1] in den Fluoreszenzspektren des 1,3-Diphenylpropans und einiger seiner Derivate mit Sicherheit nachgewiesen. Bereits früher hatten YANARI, BOVEY und LUMRY [2] vermutet, die anomale Fluoreszenz von Polystyrol könne auf Excimerbildung beruhen. Seither wurde diese Fluoreszenz, die im Gegensatz zur gewöhnlichen Excimerfluoreszenz von der Konzentration der Lösung unabhängig ist, an mehreren monomeren und polymeren Verbindungen beobachtet [3–6].

Im Rahmen von Untersuchungen über die Fluo-

Sonderdruckanforderungen an Dr. W. KLÖPFFER, Battelle-Institut e. V., Hauptabteilung Chemie, *D-6000 Frankfurt (Main)*, Postfach 900 160.

[1] FUMIO HIRAYAMA, J. Chem. Phys. **42**, 3163 [1965].
[2] S. S. YANARI, F. A. BOVEY u. R. LUMRY, Nature London **200**, 242 [1963].
[3] M. T. VALA JR., J. HAEBIG u. S. A. RICE, J. Chem. Phys. **43**, 886 [1965].
[4] J. W. LONGWORTH u. F. A. BOVEY, Biopolymers **4**, 1115 [1966].
[5] J. W. LONGWORTH, Biopolymers **4**, 1131 [1966].